ECS Transactions, 50 (2) 87-98 (2012)
10.1149/05002.0087ecst ©The Electrochemical Society

Modeling Oxygen Concentration Oscillation in the Gas channel of Polymer Electrolyte Fuel Cells: a Comparison between Numerical and Analytical Approaches

Philipe GUILLEMET[a], Gaël MARANZANA[b,c], Julia MAINKA[b,c], Adrien LAMIBRAC[b,c], Jérôme DILLET[b,c], Olivier LOTTIN[b,c].

[a] L'UNAM, Ecole polytechnique de l'université de Nantes, IMN, CNRS, Nantes, France
[b] LEMTA, Université de Lorraine, Vandoeuvre-lès-Nancy, France
[c] LEMTA, CNRS, Vandoeuvre-lès-Nancy, France

Considering the complexity of the electrical behavior (polarization curve and impedance spectrum) of PEFC and the lack of relevant models that could be used to identify the main transport parameters in Membrane Electrode Assemblies (MEA), a semi-analytical pseudo-bidimensionnal model is currently developed. Its main characteristics are first recalled. Then the results of a full numerical two-dimensional model are compared to those of the pseudo-bidimensionnal approach and analyzed. It is shown that oxygen diffusion inside the GDL can be considered as a 1D diffusion without any appreciable discrepancy and that the electrode can be modeled as a plane without major error either on impedance spectrum or polarization curve. Oxygen diffusion through the gas channel reveals an important discrepancy between volumetric and plane descriptions, leading to the necessity of a more complex model of the fluid flow in the gas channel.

Introduction

Electrochemical Impedance spectroscopy (EIS) is widely used for analyzing the operation of Polymer Electrolyte Fuel Cells (1). However, the interpretation of the two arcs that appear generally in Nyquist plots (in the case of PEFCs fed with air) can be difficult in the absence of clearly validated models. Indeed, the most widely encountered approaches are mono-dimensional and they rely on the Randles equivalent circuit that associates the high frequency loop to capacitive, kinetic, as well as charge transport effects (2) and the low frequency loop to oxygen transport (3, 4). However, Schneider et al. showed clearly that the local spectra of air-fed PEFC (i.e., the impedance spectra measured locally along the air channel) are coupled to the transport of oxygen along the air channel (5, 6). Nevertheless, these results confirm also the complexity of the electrical behavior of PEFC and the lack of relevant models that could be used -for instance- to identify the main transport parameters at stake in Membrane Electrode Assemblies (MEA). In parallel with the works of Schneider et al., Kramer et al. (7) presented briefly a full numerical two-dimensional model that confirmed, at least qualitatively, the experimental results. On the other hand, we developed recently a semi-analytical model (7-9) which main characteristics are recalled in the first section of the paper. This model enables us to calculate recursively the fuel cell impedance (for a constant in time air flow) by considering the effects of oxygen depletion and concentration oscillations along

the air channel. Yet, this model is based on simplifying assumptions that require to be validated. This constitutes the main objective of this work. For this, we compare the results of a full numerical two-dimensional model to those of this pseudo-bidimensional approach.

Full 2D model, numerical solving

The geometry is shown in Figure 1. It includes a membrane, a cathode electrode, a gas diffusion layer and a gas channel, all in 2D rectangular shape. The values of the model parameters are given in Table I. Oxygen is supplied at the upper side of the channel at constant concentration in a water saturated air flow. The gas diffuses and flows along the channel and diffuses through the gas diffusion layer up to the whole thickness of the electrode where oxygen is consumed in the redox reaction.

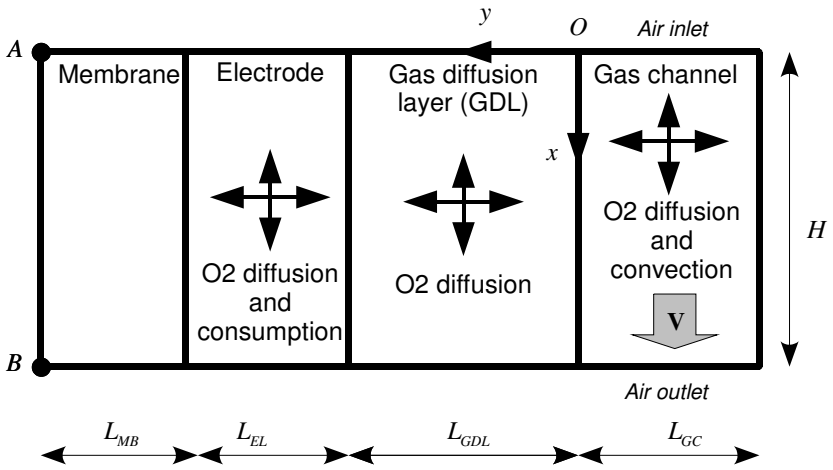

Figure 1. 2D model geometry.

The main hypotheses are the following: (i) the anode is neglected, (ii) the electrode is assumed to obey a Tafel kinetic, (iii) the electronic potential is assumed uniform along the Ox and Oy directions in both membrane and electrode, (iv) the cell voltage U is assumed uniform along the Ox direction, (v) the diffusion of oxygen is Fickian in each domain with the same effective diffusion coefficient D, (vi) the air flow velocity V is assumed constant in space and time along the channel. The value of this velocity is chosen as a function of the air stoechiometry at the channel inlet. Finally, for the sake of simplicity, the membrane protonic conductivity σ_m, the Tafel slope b, the oxygen effective diffusion coefficient D and the cathode double layer capacitance C_{dl} are considered as uniform.

The charge transport in the membrane is described by Ohm's law without current source:

$$\nabla\Phi_p(x,y,t) = -\frac{1}{\sigma_m} J(x,y,t) \qquad \nabla J(x,y,t) = 0 \qquad [1]$$

where Φ_p is the protonic potential inside the membrane, σ_m is the membrane protonic conductivity and J is the local protonic current density. At the membrane left boundary, the cell potential (U_0) is imposed.

Inside the electrode, the charge transport is described as depicted in the agglomerate model (2), according to the Transmission Line Model (TLM, (5)):

$$\nabla \Phi_p(x,y,t) = -\frac{1}{\kappa} J(x,y,t) \quad [2]$$

where κ is the protonic conductivity inside the electrode. The local variation of the current density is related to the double layer charge storage and to the faradic current of the redox reaction occurring in the electrode:

$$\nabla J(x,y,t) = -c_{dl} \frac{\partial \Phi_p(x,y,t)}{\partial t} + j_f(x,y,t) \quad [3]$$

where c_{dl} is the double layer volumetric capacitance ($c_{dl} = \frac{C_{dl}}{L_{EL}}$, with C_{dl} the surface double layer capacitance) and j_f is the volumetric faradic current from the redox reaction between oxygen and hydrogen protons written in the high electrode potential regime:

$$j_f(x,y,t) = J_0 \cdot S_f \cdot \frac{c_{O2}(x,y,t)}{c_0} \cdot \left[\exp\left(\frac{\eta(x,y,t)}{b} \right) \right] \quad [4]$$

In equation [4], J_0 is the exchange current density of the redox reaction, S_f is a roughness scale factor taking into account the total exchange surface per unit volume inside the electrode porosity, c_{O2} is the local oxygen concentration, c_0 is the reference concentration of oxygen and b is the Tafel slope.

The potential evolution equation is a diffusion-type equation, obtained by coupling equations [2] and [3] :

$$c_{dl} \frac{\partial \Phi_p(x,y,t)}{\partial t} - \kappa \Delta \Phi_p(x,y,t) = j_f(x,y,t) \quad [5]$$

Mass transport through the electrode and the GDL is purely diffusive:

$$\frac{\partial c_{O2}(x,y,t)}{\partial t} - D \cdot \Delta c_{O2}(x,y,t) = Q(x,y,t) \quad [6]$$

where D is the effective mass diffusion coefficient and $Q = \frac{j_f}{4 \cdot F}$ is the volumetric mass source / sink in the electrode ($Q = 0$ in the GDL).

In the channel, the mass transport model is completed with a uniform velocity convection term along the *Oy* direction:

$$\frac{\partial c_{O2}(x,y,t)}{\partial t} - D \cdot \Delta c_{O2}(x,y,t) + \mathrm{V} \cdot \nabla c_{O2}(x,y,t) = 0 \qquad [7]$$

where the flow velocity V is related to the oxygen stoichiometric coefficient S_{O2} by $V = S_{O2} \frac{\langle J \rangle_{x,t} \cdot H}{4F \cdot c_0 \cdot L_{GC}}$, where $\langle J \rangle_{x,t}$ is the space average value of the current density, F is the Fadaray constant, H is the gas channel length, L_{GC} is the gas channel width and c_0 is the air inlet oxygen concentration:

$$c_0 = 0.21 \cdot \frac{p}{R \cdot T} \cdot \left(1 - \frac{p_{sat}}{p}\right) \qquad [8]$$

In equation [8] p_{sat} is the vapor saturation pressure that depends only on the temperature T, p is the gas pressure and R is the universal gas constant. At the inlet boundary of the channel, the oxygen concentration is imposed.

The principle of EIS consists in adding a small sinusoidal perturbation to a steady state signal. Each variable X can thus be decomposed into a steady state $\langle X \rangle_t$ and a sinusoidal component of amplitude δX : $\bar{X} = \langle \bar{X} \rangle_t + \delta X \cdot \exp(i \cdot \omega \cdot t)$ where $\omega = 2\pi \cdot f$ is the pulsation (f is the frequency) and $i^2 = -1$. In the continuation, the overline denoting complex numbers is omitted to simplify the notation. Because the mean value of each model variable satisfies the corresponding steady state equation, each domain and boundary equation can be expressed in term of parameter variation. The charge transport in the membrane is then described by:

$$\nabla \delta\Phi_p = -\frac{1}{\sigma_m} \delta J \qquad \nabla \delta J = 0 \qquad [9]$$

In the electrode, the domain equations are:

$$\begin{aligned} &\nabla \delta J = -i \cdot \omega \cdot c_{dl} \cdot \delta\Phi_p + \delta j_f \\ &i \cdot c_{dl} \cdot \omega \cdot \delta\Phi_p - \kappa \cdot \Delta\delta\Phi_p = \delta j_f \\ &\delta j_f = J_0 \cdot S_f \cdot \left[\frac{\delta c_{O2}}{c_0} + \frac{c_{O2}}{c_0} \frac{\delta\Phi_p}{b} \right] \cdot \exp\left(\frac{\Phi_p}{b} \right) \end{aligned} \qquad [10]$$

The mass transport equations are the following, coming from equation [6] and [7]:

$$i \cdot \omega \cdot \delta c_{O2} - D \cdot \Delta\delta c_{O2} = 0 \quad \text{(in electrode)} \qquad [11]$$

$$i \cdot \omega \cdot \delta c_{O2} - D \cdot \Delta\delta c_{O2} = \frac{\delta j_f}{4 \cdot F} \quad \text{(in gas diffusion layer)} \qquad [12]$$

$$i \cdot \omega \cdot \delta c_{O2} - D \cdot \Delta\delta c_{O2} + \mathrm{V} \cdot \nabla \delta c_{O2} = 0 \quad \text{(in gas channel)} \qquad [13]$$

A full numerical method is choosen to solve this system of coupled partial differential equations using finite element method in Comsol / Matlab environnement.

Pseudo 2D model, semi-analytical solving

The geometry of this model is shown in Figure 2. It includes a rectangular shape 2D gas diffusion layer. The electrode and the membrane are considered as a plane boundary on the left of the GDL, as well as the gas channel on the right side. The dimension values are the same as for the full 2D model.

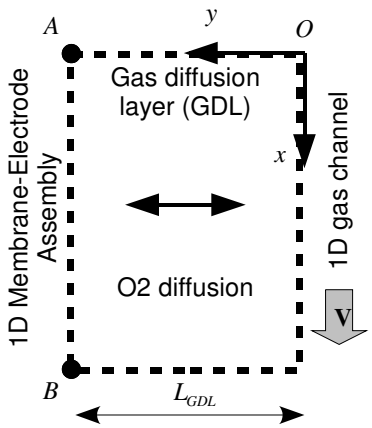

Figure 2. Pseudo 2D model geometry.

The hypotheses of this model are the same as those of the full 2D model, but the simplification of the geometry implies that:

- There is no oxygen diffusion along the Ox axis inside the channel or inside the electrode, meaning that the oxygen concentration depends only on the position y along the Oy axis.
- There is no depletion along the Ox axis inside the electrode, meaning that the protonic potential Φ_p depends only on the position y along the Oy axis. This is not the case in the full 2D model because of the finite value of the protonic conductivity through the electrode thickness.

Due to these simplifications, the electrical equations in the membrane-electrodes assembly are:

$$\begin{aligned} U(t) &= E_0 - R_{hf} \cdot J(x,t) - \Phi_p(x,t) \\ J_f(x,t) &= J_0 \cdot \frac{c_{O2}(x,-L_{GDL}t)}{c_0} \cdot \left[\exp\left(\frac{\Phi_p(x,t)}{b} \right) \right] \\ J(x,t) &= J_f(x,t) + C_{dl} \frac{\partial \Phi_p(x,t)}{\partial t} \end{aligned} \qquad [14]$$

Where R_{hf} is the high frequency surface resistance, related to the protonic membrane conductivity used in the full 2D model by equation [15]:

$$R_{hf} = \frac{L_{MB}}{\sigma_M} \quad [15]$$

Inside the GDL, the mass transport model is the same as for the full 2D model:

$$\frac{\partial c_{O2}(x,y,t)}{\partial t} - D \cdot \Delta c_{O2}(x,y,t) = 0 \quad [16]$$

but a flux-type boundary condition must be taken into account here:

$$-D \left. \frac{\partial c_{O2}}{\partial x} \right|_{y=-L_{GDL}} = \frac{J_j(x,t)}{4 \cdot F} \quad [17]$$

At the channel interface ($y = 0$), equation [18] relates the oxygen flux along the channel to the oxygen flux through the diffusion medium:

$$\frac{\partial c_{O2}}{\partial t}(x, y=0, t) + V \frac{\partial c_{O2}}{\partial x}(x, y=0, t) = \frac{D}{L_{GC}} \frac{\partial c_{O2}}{\partial y}(x, y=0, t) \quad [18]$$

To the best of our knowledge, there is unfortunately no analytical solution for this system, from equation [14] to equation [18]. A semi analytical solving method has been used to solve the equation system, fully described in (9).

Comparison between pseudo 2D and full 2D model

For each model, a polarization curve and an impedance spectrum are computed at two different points: A for the inlet and B for the outlet (see Figure 1 and Figure 2).

Code validation

In order to validate the two approaches, the polarization curves and the impedance spectra obtained with the two models (full 2D with numerical solving and pseudo 2D with semi analytical solving) have been compared in a similar case. For this purpose, the widths of the electrode and of the gas channel have been set to a very low value in the full 2D model (less than 1µm in the present case), thus simulating a 1D behavior. A good agreement has been found, the remaining discrepancy (less than 1.5% of the maximum value of each curve) being due to the nature of the solvers algorithm (Levenberg-Marquardt algorithm for a finite difference scheme using Matlab® for the pseudo-2D model, Mumps algorithm for a finite element method using Comsol® for the full 2D model). This fully validates both codes.

1D oxygen diffusion hypothesis

In order to test the 1D oxygen diffusion hypothesis in the pseudo 2D model, polarization curve and impedance spectra from the two codes have been compared, in the configuration described in Figure 3. As previously observed, no significant discrepancy has been observed over a range of oxygen effective diffusion coefficients comprised

between $D = 10^{-5}\ m^2.s^{-1}$ and $D = 10^{-8}\ m^2.s^{-1}$. This observation is mainly explained by the high value of the geometrical shape factor of the diffusing medium ($H/Lgdl = 750$) and by the weak concentration gradient along Ox axis ($\frac{\Delta c_{O2}}{\Delta x} = \frac{c_0}{2H} \approx 10\ mol.m^{-4}$ for $D = 10^{-6}\ m^2.s^{-1}$) compared to the concentration gradient along Oy axis ($\frac{\Delta c_{O2}}{\Delta y} = \frac{c_0}{L_{gdl}} \approx 1.5 \times 10^4\ mol.m^{-4}$ for $D = 10^{-6}\ m^2.s^{-1}$ and for a stoechiometry $S_{O2} = 2$). In the GDL, diffusion occurs almost solely in the Oy direction, which fully validates the 1D diffusion hypothesis of the pseudo 2D model.

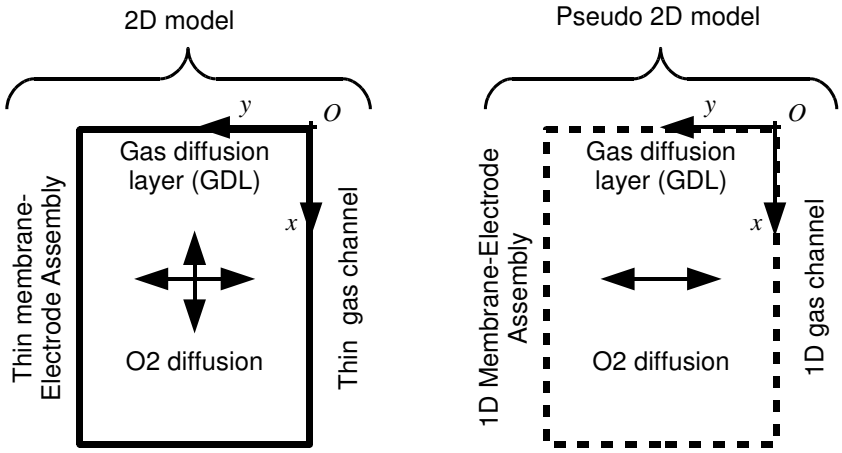

Figure 3. 2D code setup for 1D oxygen diffusion hypothesis validation. The thin gas channel in the 2D model is numerically equivalent to the 1D gas channel in the pseudo 2D model.

Plane electrode hypothesis

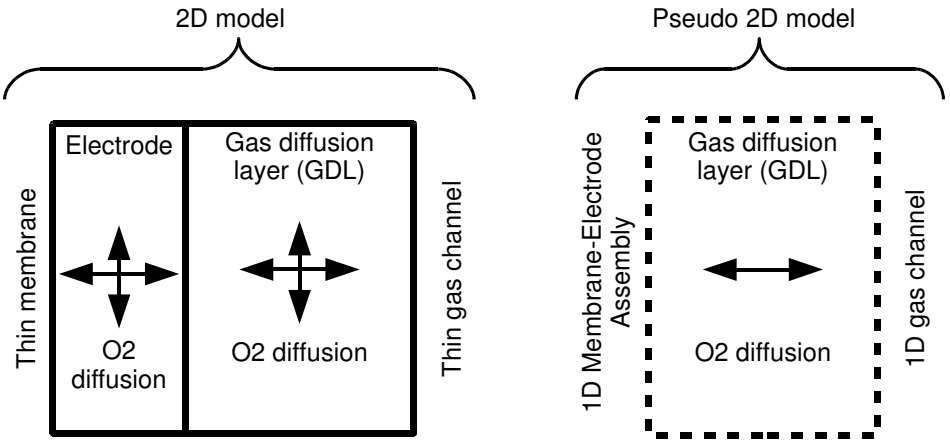

Figure 4. 2D code setup for plane electrode hypothesis testing. The thin gas channel in the 2D model is numerically equivalent to the 1D gas channel in the pseudo 2D model.

In order to test the plane electrode hypothesis of the pseudo 2D model, the 2D model is set up as described in Figure 4 : the only significant difference between the two models is the thickness of the electrode, set to 15 µm and then to 30 µm.

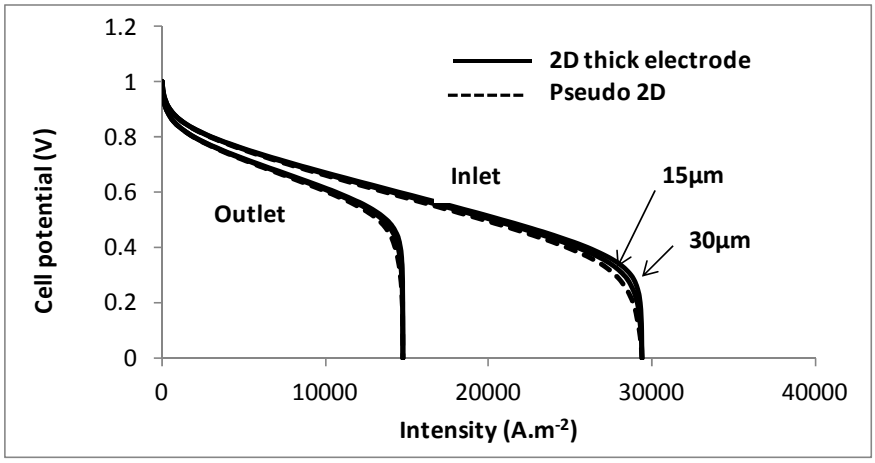

Figure 5. Polarization curve for 2D thick electrode model and pseudo 2D model. "Inlet" corresponds to point A in Figure 1 and Figure 2 "Outlet" corresponds to point B on same figures.

In Figure 5 and Figure 7 the 2D model results are given using two different widths of the electrode, every other parameters value being identical to the pseudo 2D model. It can be seen that taking into account the thickness of the electrode in the model has a weak impact on the polarization curve by comparison with a plane electrode model. The difference is nearly null at the gas channel inlet. Figure 6 shows the origin of the discrepancy between the plane and thick electrode models: the plane electrode model leads to a 0.217V potential value, while the thick electrode model leads to a non uniform potential, because of the finite protonic conductivity trough this layer. In the case of a 30µm electrode, the potential decreases from 0.224V to 0.207V.

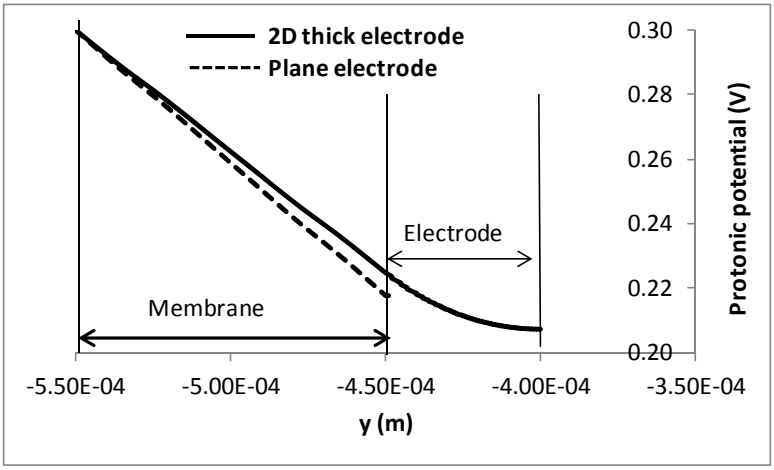

Figure 6. Protonic potential inside membrane and electrode, for a 30µm electrode thickness.

This influence of the electrode thickness is more important regarding the shape of the spectra. As expected, one can see that the high frequency part of the spectra is linear in the case of the thick electrode model. Its slope is equal to 1, characteristic value of the 1D

diffusion potential inside the electrode as a consequence of the electrical model of the electrode porous layer (5). As detailed in (6) this leads to a translation of the spectrum, from the plane model to the volumetric model, along the real axis, of a quantity given by $Z_{RD} = \frac{L_{EL}}{3\kappa}$. For a 30µm electrode, the corresponding value is $Z_{RD} = 10^{-6}\Omega.m^2$.

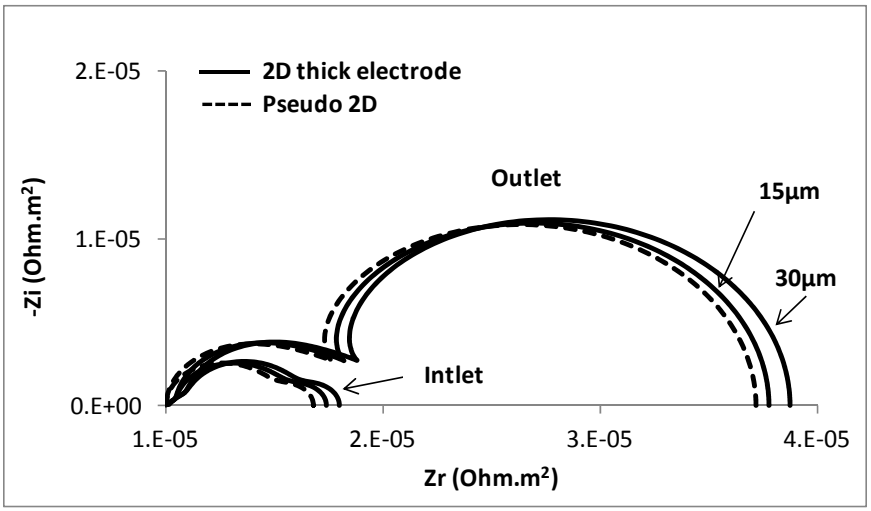

Figure 7. Impedance spectra for 2D thick electrode model and pseudo 2D model. "Inlet" corresponds to point A in Figure 1 and Figure 2, "Outlet" corresponds to point B on same figures.

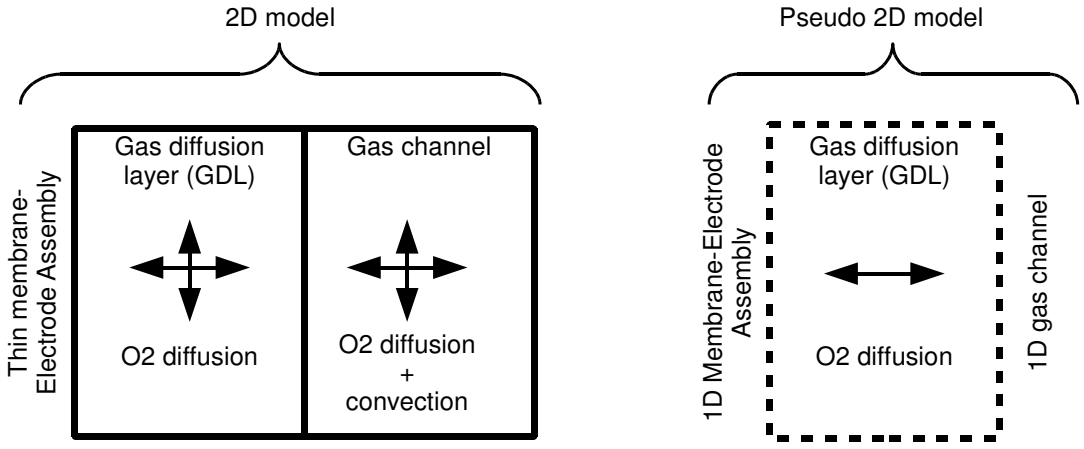

Figure 8. 2D code setup for 1D channel hypothesis testing.

1D channel hypothesis

In order to test the 1D gas channel hypothesis of the pseudo 2D model, the 2D model is set up as described in Figure 8: the only significant difference between the two models is the thickness of the gas channel, set to 700 µm for the 2D model. It can be seen, in Figure 9 and Figure 10, that this thickness has no significant influence on the electrical behavior at the gas inlet, neither on the polarization curve nor on the impedance spectra. This is clearly related to the distribution of oxygen concentration in the gas channel. Both

the 2D and pseudo 2D models consider the same concentration (c_0) at the gas inlet ($x = 0$): no diffusion occurs along the Oy axis (the concentration gradient $\frac{\partial c_{O2}}{\partial y}$ is equal to zero) at this location.

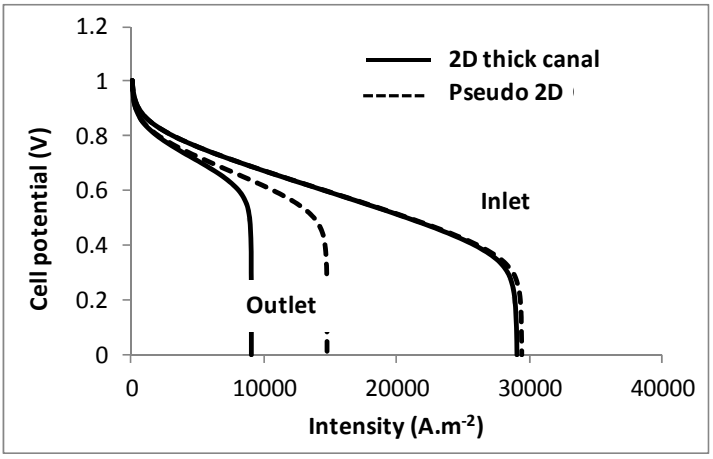

Figure 9. Polarization curve for 2D thick canal model and pseudo 2D model. "Inlet" corresponds to point A in Figure 1 and Figure 2, "Outlet" corresponds to point B in the same figures.

In contrast to this observation, an important discrepancy can been seen at the outlet of the channel, as much in the polarization curve as in the impedance spectrum. The physical origin of this discrepancy can be found again in the oxygen concentration profile : at the outlet of the air channel ($x = 0.3\,m$), the concentration gradient in the 2D channel is $\frac{\partial c_{O2}}{\partial y} = 473\,mol.m^{-4}$, leading to a diffusion resistance that limits the current and increases the impedance at this location. It must be noted that for these numerical simulations, identical values of the oxygen diffusion coefficient in the air channel and in the gas diffusion layer are used. This hypothesis seems reasonable since the porosity of the gas diffusion layer being quite high, the actual difference between both values is most probably low and not significant. On the other hand, we considered a plug flow in the air channel, and thus slightly underestimated the value of the oxygen mass transport resistance. It could be more appropriate to consider a parabolic velocity profile (7) but it must be kept in mind that the air flow is actually much complex, with the presence of water droplets and probably a significant part of the gas flowing in the gas diffusion layer, either below the channel rib (in the case of a serpentine flow field) or parallel to the main flow (12).

Modeling the complexity of the actual air flow is out of the scope of this paper, but considering its exact nature would obviously have an important effect on the impedance. For instance, dispersion along the channel direction (i.e. effective diffusion induced by convection) would probably tend to smooth the oxygen concentration oscillations and to reduce the low frequency impedance near the outlet. Further analysis attempting to characterize the flow, for example by the mean of dispersion coefficients along the two directions has to be held.

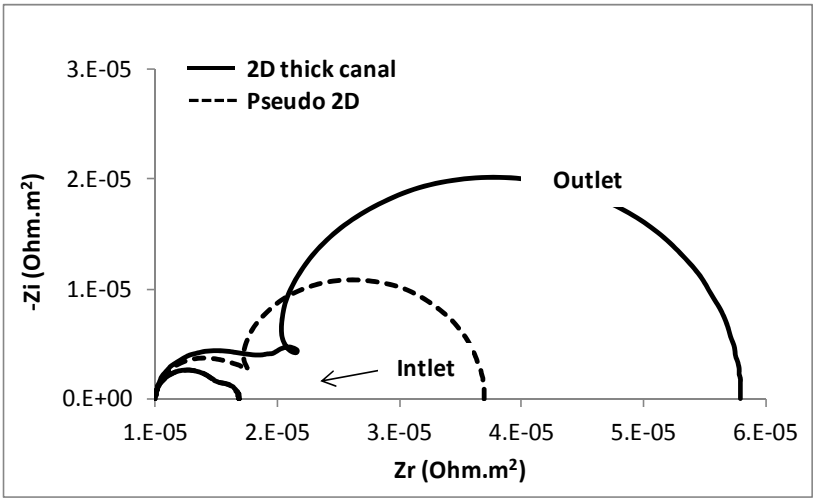

Figure 10. Impedance spectrum for 2D thick canal model and pseudo 2D model. "Inlet" corresponds to point A in Figure 1 and Figure 2, "Outlet" corresponds to point B in the same figures.

Conclusion

The comparison between a full 2D model and a pseudo 2D model of the whole electrode - GDL - gas channel system in different configurations shows that in the chosen numerical conditions:

- Oxygen diffusion inside the GDL can be considered as 1D diffusion in the *Oy* direction without any appreciable consequence because of the high shape factor value and of the low *Ox* direction concentration gradient.
- The electrode can be modeled as a plane without any major error, either on the impedance spectra or polarization curves, provided that its actual thickness remains below 15 µm. For a thicker electrode, a discrepancy between the plane electrode model and the volumetric electrode model appears in the impedance spectrum. This discrepancy is essentially due to a translation at high frequencies of the real part of the impedance due to the potential diffusion through the electrode.
- Oxygen diffusion through the gas channel along the *Oy* direction reveals an important discrepancy between volumetric and plane descriptions, leading to the necessity of a more complex model of the fluid flow in the gas channel.

Beyond the clarification that this kind of model provides concerning the computation and the analysis of both PEM polarization curves and impedance spectra, the characterization of coupled mass transport limitations due to the channels flow and to the MEA thickness needs coupled efforts from modeling and experimental approaches.

Numerical values

TABLE I. Notation and model parameters values.

Quantity	Notation	Value	Unit
Effective oxygen diffusion coefficient	D	5×10^{-6}	$m^2.s^{-1}$
Cell open circuit voltage	E_0	1	V
Faraday number	F	96485	$C.mol^{-1}$
Channel length	H	0.3	m
Exchange current density	J_0	5×10^{-3}	$A.m^{-2}$
Absolute air pressure	p	1	Atm
High frequency resistance	R_{hf}	0.1	$Ohm.cm^2$
Ideal gas constant	R	8.31	$J.mol^{-1}.K^{-1}$

References

1. J. R. Mac Donald, *Impedance Spectroscopy*, John Wiley and Sons (1987).
2. M. Eikerling and A. A. Kornyshev, *J. Electroanalytical Chem.*, **475**, 107 (1999).
3. Y. Bultel, K. Wiezell, F. Jaouen, P. Ozil and G. Lindbergh, *Electrochimica Acta*, **51**, 474 (2005).
4. T. E. Springer, T. A. Zawodzinski, M. S. Wilson and S. Gottesfeld, *J. Electrochem. Soc.*, **143**, 587 (1996).
5. R. de Levie, *Electrochimica Acta*, **8**, 751 (1963).
6. B. E. Conway, *Electrochemical Supercapacitors, Scientific Fundamentals and Technological Applications*, New York (1999).
7. D. Kramer, I. A. Schneider, A. Wokaun and G. G. Scherer, *ECS Trans.*, **3**, 1249 (2006).
8. I. A. Schneider, S. A. Freunberger, D. Kramer, A. Wokaun and G. G. Scherer, *J. Electrochem. Soc.y*, **154**, B383 (2007).
9. G. Maranzana, J. Mainka, O. Lottin, J. Dillet and A. Lamibrac, *Electrochimica Acta*, Submitted (2012).
10. J. Mainka, G. Maranzana, J. Dillet, S. Didierjean and O. Lottin, *ECS Trans.*, **19**, 33 (2009).
11. J. Mainka, Impédance locale dans une pile à membrane H2 / air, in *PhD Thesis*, Nancy, France (2011).
12. D. Conteau, C. Bonnet, D. Funfschilling, M. Weber, S. Didierjean and F. Lapicque, *Fuel Cells*, **10**, 520 (2010).